Isotope shifts and fine structures of ^{6,7}Li *D* lines and determination of the relative nuclear charge radius

G. A. Noble, B. E. Schultz, H. Ming, and W. A. van Wijngaarden*
Physics Department, Petrie Building, York University, 4700 Keele Street, Toronto, Ontario, Canada M3J 1P3
(Received 20 March 2006; published 11 July 2006)

The ^{6,7}Li *D* lines were excited using an electro-optically modulated cw dye laser that intersected an atomic beam. Fluorescence was recorded as the laser was scanned across the resonance. Hence each transition was multiply excited allowing for calibration of the frequency scan. The ^{6,7}Li $2P$ fine structures were found to be $10\,052.964\pm0.050$ and $10\,053.119\pm0.058$ MHz. The $D1$ and $D2$ isotope shifts were determined to be $10\,534.039\pm0.070$ and $10\,534.194\pm0.104$ MHz. The latter imply values for the ^{6,7}Li relative nuclear charge radius that are within 20×10^{-3} fm of each other, which is consistent with the estimated uncertainties.

DOI: 10.1103/PhysRevA.74.012502 PACS number(s): 31.30.Gs, 32.10.Fn

I. INTRODUCTION

Recent advances in experiment and theory have made possible the determination of relative nuclear sizes with accuracies of less than 0.1 fm, exceeding that obtained in conventional nuclear scattering experiments [1,2]. Lithium is of special interest given that highly accurate theoretical estimates of energy levels can now be made for this three-electron system using the Hylleraas variational technique [3–6]. Nearly all of the experiments have measured isotope shifts of transitions in either singly ionized or neutral ^{6,7}Li [1,7]. These results combined with theory have yielded values of the lithium nuclear charge radius permitting tests of nuclear models [8,9]. Recently, theoretical work in combination with experimental measurements of isotope shifts found that the charge radius decreases with increasing neutron number in ^{6,7,8,9}Li [10].

This experiment reports a study of the *D*-line transitions in ^{6,7}Li. The fine structure and isotope shifts of the $2S_{1/2}$-$2P_{1/2,3/2}$ transitions have been found by a number of experiments [7]. The values for the nuclear sizes as determined from the $D1$ and $D2$ isotope shifts have not always been mutually consistent [1]. A difficulty encountered in experiments that scan a laser frequency across the resonance is proper calibration of the étalon used to monitor the change in laser frequency. Such calibrations can be readily done using a femtosecond frequency comb [11], but various effects such as vibrations, temperature fluctuations, etc., can perturb the étalon, causing erroneous results [12].

This experiment used a technique whereby a frequency-modulated laser beam excited an atomic beam [13,14]. Each transition generated multiple peaks separated by the laser modulation frequency as the laser was scanned across the resonance. Each laser scan was then calibrated using the modulation frequency which was specified by a frequency synthesizer. The results for the ^{6,7}Li $2P$ fine structures agree with the most accurate data previously obtained using a variety of experimental techniques [1,7], while the values for the nuclear charge radius of ^{6}Li found using the $D1$ and $D2$ isotope shifts are mutually consistent.

*Corresponding author. Electronic address: wlaser@yorku.ca

II. EXPERIMENT

The apparatus is a refinement of that used in an earlier experiment and is therefore only briefly described [15]. An atomic beam consisting of either pure ^{6}Li or natural lithium (92.5% ^{7}Li) was generated by heating a lithium sample in an oven to a few hundred degrees centigrade. The oven was housed in a vacuum chamber pumped to a pressure of 1×10^{-7} torr. Light, resonant with the $2S_{1/2}$-$2P_{1/2,3/2}$ transitions at 670 nm, illustrated in Fig. 1, was generated by a ring

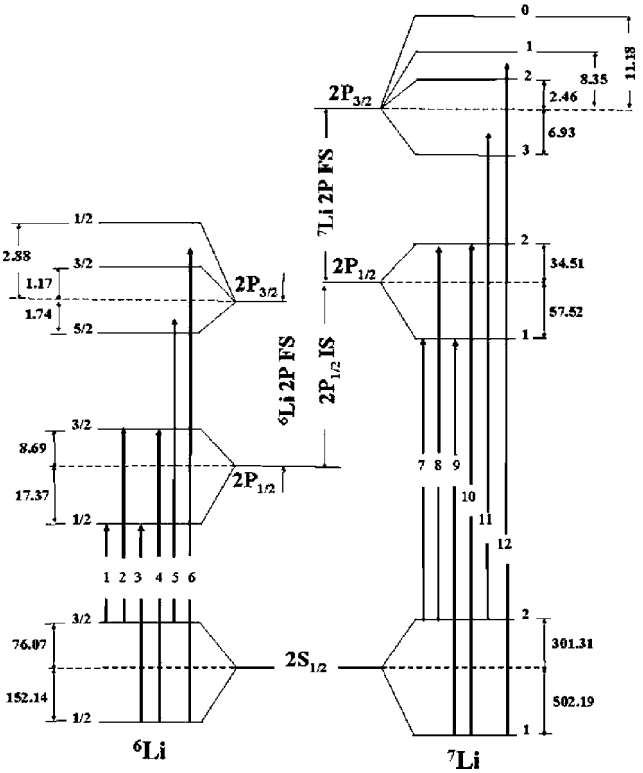

FIG. 1. Relevant lithium energy levels. The frequency intervals listed in units of MHz are taken using data found in the literature [17,18]. The vertical energy axis is not drawn to scale. The positions of the various hyperfine levels are indicated relative to the center of gravity energy of a state $E_{cg}=\Sigma_F(2F+1)E_F/\Sigma_F(2F+1)$, where E_F is the energy of the hyperfine level F.

dye laser (Coherent 699) which can be scanned for up to 30 GHz. The laser beam was linearly polarized and passed through an electro-optic modulator (New Focus 4851) operating at either 6.8 or 9.2 GHz. The modulation frequency was generated by a frequency synthesizer with an accuracy of better than 3 parts in 10^7.

The laser and atomic beams intersected orthogonally to minimize the first-order Doppler shift. This intersection region was surrounded by three pairs of Helmholtz coils that reduced the Earth's magnetic field to less than 20 mG. Fluorescence emitted in the direction perpendicular to both the laser polarization and propagation directions was detected by a photomultiplier (Hamamatsu R928).

The experiment was designed with a number of significant improvements over that done previously [15]. The dye laser had a linewidth of only 0.5 MHz and has a much more linear scan than the diode laser used earlier. Each laser scan was monitored by passing part of the laser beam through a confocal Fabry-Perot étalon (Burleigh CFT-500). This interferometer had a free spectral range of nearly 150 MHz, which was half that of the étalon previously employed. The times for the laser frequency to change by one free spectral range at the beginning and end of a 15-GHz scan differed by less than 1%. Hence the nonlinearity of the laser scan during a single 150-MHz free spectral range interval was estimated to be less than 1 part in 10^4.

The second major improvement was the use of a digital oscilloscope (Tektronix TDS 5054 B) that recorded both the fluorescence photomultiplier signal as well as the transmission of the laser through the étalon. Data were recorded at a rate of 4000 Hz, and each point represented a frequency interval of about 12 kHz as compared to about 0.5 MHz, previously. This permitted a much more detailed examination of the transition lineshapes.

Nearly 600 laser scans were recorded. About half of the scans were taken using pure ^{6}Li as shown in Fig. 2, where the laser was frequency modulated at 6.8 GHz. The remaining runs used natural lithium, and a sample run is shown in Fig. 3. During each run, the photomultiplier voltage was adjusted to avoid saturating the detector signal. The laser power was varied between 0.05 and 1.5 mW using neutral density filters, to check that the results were independent of laser power.

The data were analyzed using MATLAB 7.0. The fluorescence peak positions were found by fitting a sum of Lorentzian functions to the peaks in the spectrum. Each Fabry-Perot transmission maxima was found by averaging the positions on either side of the peak where the transmitted laser intensity was half of the maximum peak intensity. The position of each fluorescence peak relative to the nearest Fabry-Perot peak was then determined using a fifth-order polynomial to interpolate between the six nearest Fabry-Perot peak centers to account for any nonlinearity of the laser frequency scan. The free spectral range of the étalon was determined using the electro-optic modulation frequency intervals as shown in Figs. 2 and 3.

III. RESULTS AND CONCLUSIONS

The experiment was tested by comparing the measured results for the ground- and excited-state hyperfine intervals

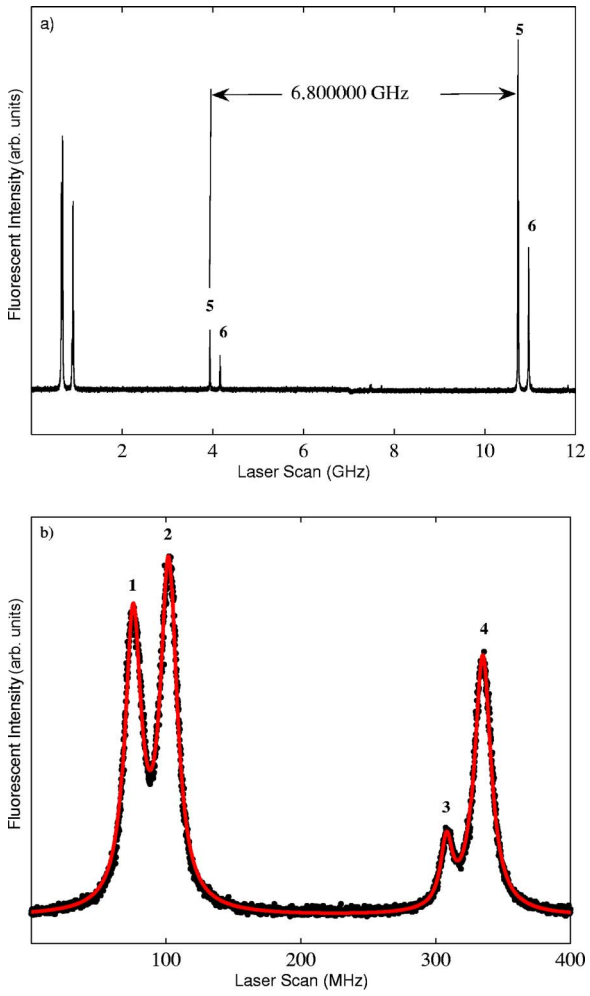

FIG. 2. (Color online) Sample ^{6}Li laser scan. (a) Shows a scan where the laser excited transitions 1–6 illustrated in Fig. 1 using an electro-optic modulation frequency of 6.800000 GHz. The first four peaks are shown distinctly in (b) along with the red curve fitted to the data as is discussed in the text.

to published values. The ^{6}Li $2S_{1/2}$ hyperfine splitting which equals the intervals separating peaks 1 and 3, and also peaks 2 and 4, was measured to be 228.182 ± 0.086 MHz. The uncertainty represents one standard deviation of the data from the average value. This agrees very well with the value of 228.205 259 MHz obtained using the atomic beam magnetic resonance method (ABMR) [16]. Similarly, the ^{7}Li $2S_{1/2}$ hyperfine splitting which equals the frequency interval separating peaks 7 and 9, and also 8 and 10, was found to be 803.544 ± 0.066 MHz, which is consistent with the ABMR result of 803.504 087 MHz [16]. The hyperfine splitting of the excited $2P_{1/2}$ state was also examined yielding magnetic-dipole constants of 17.407 ± 0.037 and 45.893 ± 0.026 MHz for ^{6}Li and ^{7}Li, respectively. These values also agree with published data. Indeed, the uncertainties are comparable to the most accurate results obtained in our previous work [15] and by other groups using optical double-resonance and level crossing experiments [17].

The Li $2P$ fine structure was determined by examining the separation of the $D2$ and $D1$ transitions illustrated in Fig.

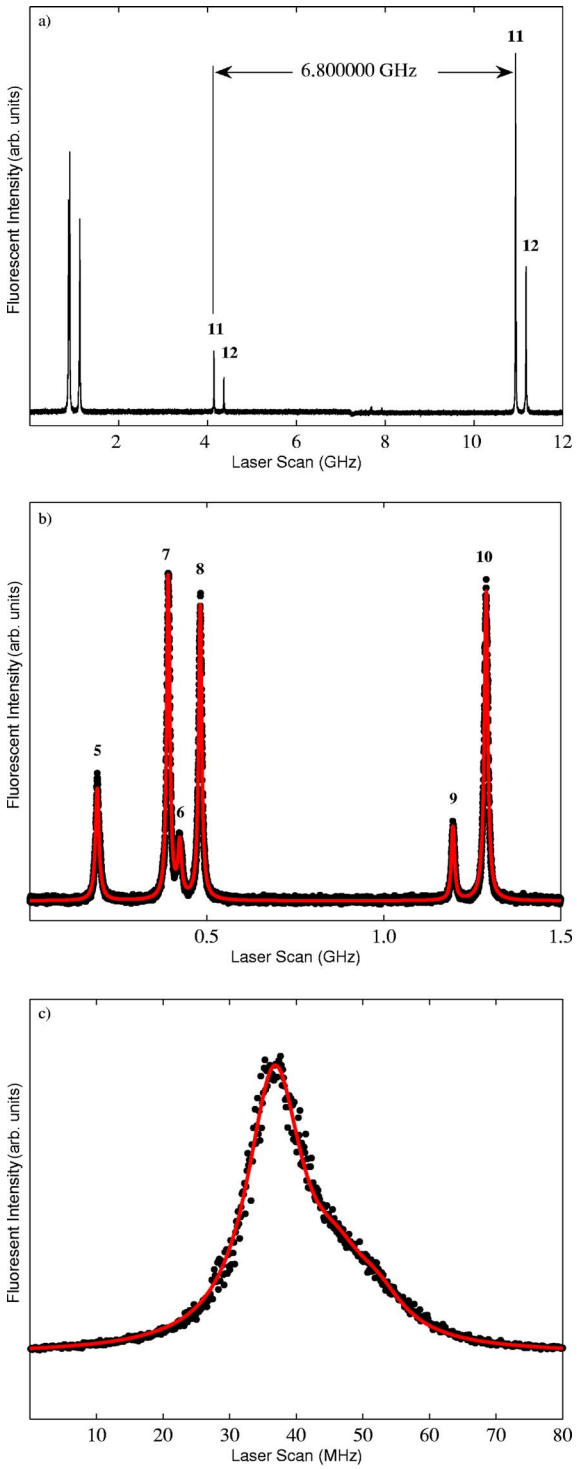

FIG. 3. (Color online) Sample natural Li laser scan. (a) Shows a scan where the laser excited transitions 5 and 6 of ^{6}Li and transitions 7–12 of ^{7}Li using an electro-optic modulation frequency of 6.80000 GHz. (b) Shows the first six peaks, while (c) shows transition 11 along with the red curves fitted to the data as is discussed in the text.

1. A complication is that the hyperfine splittings of the $2P_{3/2}$ state are less than or comparable to the 5.8-MHz full width at half maximum (FWHM) natural linewidth of the $2S$-$2P$ transition in both ^{6,7}Li. A computer program was therefore written that considered the repeated excitation and subsequent radiative emission of a fluorescent photon as the atom passed through the laser beam. The model used values for the $2P_{3/2}$ hyperfine splittings existing in the literature [17]. The fraction of the total fluorescence generated by each excited state hyperfine level was then found. These fluorescent fractions are affected by optical pumping as the linearly polarized laser beam is simultaneously in resonance with multiple hyperfine levels of the $2P_{3/2}$ state. This changes the relative populations of the ground-state magnetic sublevels having different $|m_F|$ where m_F is the magnetic sublevel quantum number. This does not affect peak 6 since it arises from excitation of the ^{6}Li $2S_{1/2}$ $F=1/2$ state. The fluorescent fractions contributing to peak 6 originating from the $2P_{3/2}$ $F=1/2$ and $3/2$ hyperfine levels were found to be 47.8% and 52.2%, respectively. This shifts peak 6 above the $2P_{3/2}$ center of gravity by 1.987 MHz, as indicated in Fig. 1. This correction changes by only 16 kHz if the natural linewidth of the transition is doubled. It should be emphasized that this shift was the only one that was estimated, whereas all other shifts used in the data analysis such as the shift of peak 5 from the $2P_{3/2}$ center of gravity were determined from experimental observation. The corresponding shift of peak 5 below the $2P_{3/2}$ center of gravity was observed for each scan by subtracting the ground-state hyperfine splitting and the aforementioned shift of peak 6 from the frequency interval separating peaks 5 and 6. The shifts of peaks 5 and 6 from the $2P_{3/2}$ center of gravity were comparable in magnitude but opposite in sign. Hence their effect was minimized by determining the ^{6}Li $2P$ fine structure by averaging the values obtained using the two peaks.

The ^{7}Li $2P$ fine structure was determined by examining the separation of peaks 11 and 12 from peaks 7–10. The fluorescence model shows that over 80% of the fluorescence generated by exciting peak 11 results from the radiative decay of the $2P_{3/2}$ $F=3$ hyperfine level. Fluorescence, produced by the decay of the $2P_{3/2}$ $F=1$, 2 levels, is responsible for the shoulder on peak 11 shown in Fig. 3(c). Peaks 11 and 12 were fitted using three Lorentzians whose relative peak centers were specified by the known hyperfine splittings and whose amplitudes were varied. For peak 12, the fluorescence fractions arising from the $F=0$, 1, and 2 hyperfine levels were predicted by the model to be 28%, 36%, and 36% respectively, which agree very well with the average observed quantities of 29%, 34%, and 37%. The two values found for the ^{7}Li $2P$ fine structure splitting using peaks 11 and 12, 10053.116 ± 0.079 and 10053.123 ± 0.086 MHz, respectively, are in excellent agreement and were averaged to give the entry listed in Table I.

Table I shows close agreement of the present results for the ^{6,7}Li $2P$ fine structure and the most accurate data obtained by level crossing [18] and optical double-resonance experiments [21]. Only the laser atomic beam measurement for the ^{6}Li fine-structure splitting is smaller than the other results. This is not altogether surprising given the difficulties in properly calibrating the étalon used to monitor the laser scan that have affected the previous determinations of the ^{7}Li fine structure [12,19,22]. Our earlier result for the ^{7}Li $2P$ fine structure differs from the present work as the original experiment had over an order of magnitude lower resolution

TABLE I. Comparison of results to published data: FM=frequency modulation, FT=Fourier transform, LAB=laser atomic beam, LABEO=laser atomic beam using electro-optic modulation, LC=level crossing, ODR=optical double resonance, FCPC=full core plus correlation, HV=Hylleraas variational calculation, and MCHF=multiconfigurational Hartree-Fock.

Quantity	Experiment (MHz)	Theory (MHz)	Technique
^{6}Li 2*P* FS	10052.76±0.22		LC [18]
	10050.2±1.5		LAB [19]
	10051.62±0.20		LAB [12]
	10053.044±0.091		LABEO [15]
	10052.964±0.050		This work
		10050.846±0.012	HV [20]
^{7}Li 2*P* FS	10053.24±0.22		LC[18]
	10053.184±0.058		ODR [21]
	10056.6±1.5		LAB [19]
	10053.2±1.4		LAB[22]
	10053.4±0.2		LAB [12]
	10052.37±0.11		LABEO [15]
	10053.119±0.058		This work
		10051.214±0.012	HV [20]
*D*1 isotope shift	10532±5		LAB [24]
	10534.3±0.3		LAB [19]
	10532.9±0.6		FM [25]
	10526±15		FT [26]
	10533.13±0.15		LAB [12]
	10533.160±0.068		LAB [27]
	10534.26±0.13		LABEO [15]
	10534.039±0.070		This work
		10528.7	MCHF [28]
		10534.31±0.68	HV [6]
		10534.12±0.07	HV [29]

which prevented a detailed examination of the *D*2 line shapes [15]. The experimental results for both lithium isotopes significantly exceed the theoretical estimate which was found using the Hylleraas variational technique [20]. The error bars of the theoretical estimates given in Table I are computational uncertainties. The theoretical calculation only considered terms in the Hamiltonian of order α^3 times the Rydberg energy, where α is the fine-structure constant. The discrepancy between theory and experiment is likely due to neglecting terms in the Hamiltonian of order α^4 which for helium contribute several MHz to the fine-structure splitting [23].

The simplest way to determine the *D*1 isotope shift is to measure the interval separating peaks 1–4 from peaks 7–10 in a scan of natural lithium. However, the ^{6}Li peaks are then more than an order of magnitude smaller than when pure ^{6}Li is used. ^{6}Li can be added to a natural lithium sample but this increases the overlap of peaks 6, 7, and 8 as shown in Fig. 3(b). The *D*1 isotope shift was instead determined by measuring the intervals separating peaks 7–10 from peak 5 in the natural lithium runs and the intervals separating peaks 1–4 from peak 5 in the ^{6}Li data runs. The *D*1 isotope shift was then found using the ^{6,7}Li ground- and excited-state hyperfine splittings. The result for the *D*1 isotope shift agrees with our earlier result, but has half the uncertainty. It also is much closer to the theoretical prediction of Yan and Drake [6,29] than the multiconfigurational Hartree-Fock calculation [28]. The *D*2 isotope shift listed in Table II for this experiment was found from the measured *D*1 isotope shift and the ^{6,7}Li fine-structure splittings as is illustrated in Fig. 1.

Table II shows how the nuclear charge radius r_c of ^{6}Li was determined from the difference of the squares of the ^{6,7}Li charge radii as given in Ref. [1]:

$$\Delta r_c^2 = r_c^2(^6\mathrm{Li}) - r_c^2(^7\mathrm{Li}) = (\delta\nu_{jk} - \delta E_{jk})/C_{jk}. \quad (1)$$

Here $\delta\nu_{jk}$ is the measured isotope shift for the transition between states j and k, δE_{jk} is the calculated isotope shift difference for the two states excluding the nuclear size correction, and C_{jk} is proportional to the square of the electron wave function at the nucleus. An important experimental test is to check whether results obtained for Δr_c^2, using isotope shifts measured for different transitions, agree. The experiments of Riis *et al.* [30], Bushaw *et al.* [27], and the present work pass this consistency check, but not those obtained by Scherf *et al.* [12]. The results of Bushaw *et al.* [27], however,

TABLE II. Determination of ^{6}Li nuclear charge radius. The measured isotope shifts are given by $\delta\nu_{jk}$, while δE_{jk} and C_{jk} were obtained by a Hylleraas variational calculation given in Ref. [1]. The first and second error bars in the columns for Δr_c^2 and $r_c(^6\mathrm{Li})$ are the total and experimental (bracketed) uncertainties.

Transition	$\delta\nu_{jk}$ (MHz)	δE_{jk} (MHz)	C_{jk}	Δr_c^2 (fm^2)	$r_c(^6\mathrm{Li})$ (fm)	Reference
$\mathrm{Li}^+(2\,^3S_1\text{-}2\,^3P_0)$	34747.73±0.55	34740.17±0.03	9.705	0.779±0.057(0.057)	2.548±0.031(0.011)	[30]
$\mathrm{Li}^+(2\,^3S_1\text{-}2\,^3P_1)$	34747.46±0.67	34739.87±0.03		0.782±0.069(0.069)	2.548±0.032(0.014)	[30]
$\mathrm{Li}^+(2\,^3S_1\text{-}2\,^3P_2)$	34748.91±0.62	34742.71±0.03		0.639±0.064(0.064)	2.520±0.031(0.031)	[30]
$\mathrm{Li}(2\,^2S_{1/2}\text{-}3\,^2S_{1/2})$	11453.95±0.13	11453.01±0.06	1.566	0.600±0.091(0.083)	2.512±0.033(0.018)	[10]
	11453.734±0.030			0.462±0.042(0.019)	2.485±0.030(0.009)	[27]
$\mathrm{Li}(2\,^2S_{1/2}\text{-}2\,^2P_{1/2})$	10533.160±0.068	10532.17±0.07	2.457	0.403±0.040(0.028)	2.473±0.030(0.008)	[27]
	10533.13±0.15			0.391±0.067(0.061)	2.470±0.032(0.014)	[12]
	10534.039±0.070			0.761±0.040(0.028)	2.544±0.030(0.006)	This work
$\mathrm{Li}(2\,^2S_{1/2}\text{-}2\,^2P_{3/2})$	10534.93±0.15	10532.57±0.07	2.457	0.961±0.067(0.061)	2.592±0.032(0.014)	[12]
	10534.194±0.104			0.661±0.050(0.042)	2.524±0.030(0.009)	This work
Nuclear theory				0.740	2.54±0.01	[9]
e-nuclear scattering				0.842	2.56±0.05	[2]

are lower than the data obtained by the other groups and also differ with data obtained in an electron nuclear scattering experiment [2] and the value predicted by nuclear theory [30].

The value of Δr_c^2 obtained by averaging the results of the experiment of Riis *et al.* [30] that studied the Li^+ $2\,^3S_1\text{-}2\,^3P_{0,1,2}$ transitions and the experiment of Ewald *et al.* [10] that examined the Li $2\,^3S_{1/2}\text{-}3\,^2S_{1/2}$ transition is 0.700 fm^2. This is in excellent agreement with the average value of our two measured values of 0.704 fm^2. However, the uncertainty of the present results is due about equally to experimental and theoretical uncertainties, whereas it is dominated by experimental effects in the other experiments. The ^{6}Li charge radius was determined using the known ^{7}Li charge radius 2.39±0.03 fm [2]. The uncertainties listed in Table II for $r_c(^6\mathrm{Li})$ are dominated by the accuracy of $r_c(^7\mathrm{Li})$. The average value of the ^{6}Li charge radius obtained by the experiments of Riis *et al.* and Ewald *et al.* of 2.532 fm is nearly identical to 2.534 fm, found by averaging the two results of the present experiment.

In conclusion, this experiment has measured the $2P$ fine-structure splitting of ^{6,7}Li. The results are in excellent agreement with those obtained using several different measurement techniques, but have significantly smaller uncertainty. Moreover, the $D1$ and $D2$ isotope shifts yielded consistent information of the relative sizes of ^{6,7}Li charge radii resolving past discrepancies, which is important for evaluating nuclear models. This work facilitates future precision measurements in neutral lithium and Li^+ of fundamental constants such as the fine-structure constant as well as the study of QED effects which can be comparable in magnitude to nuclear size corrections [1,7].

ACKNOWLEDGMENTS

The authors would like to thank L. Young of Argonne National Laboratory for the loan of the Fabry-Perot étalon and A. Madej of the National Research Council of Canada for the loan of the thick étalon used in the ring dye laser. Financial support from the Canadian Natural Science and Engineering Research Council is greatly appreciated.

[1] G. W. F. Drake, W. Nörtershäuser, and Z. C. Yan, Can. J. Phys. **83**, 311 (2005).
[2] C. W. de Jager, H. de Vries, and C. de Vries, At. Data Nucl. Data Tables **36**, 495 (1987).
[3] G. W. F. Drake and Z. C. Yan, Phys. Rev. A **46**, 2378 (1992).
[4] G. W. F. Drake, in *Long Range Casimir Forces: Theory and Recent Experiments in Atomic Systems*, edited by F. S. Levin and D. A. Micha (Plenum Press, New York, 1993), pp. 107–217.
[5] Z. C. Yan, M. Tambasco, and G. W. F. Drake, Phys. Rev. A **57**, 1652 (1998).
[6] Z. C. Yan and G. W. F. Drake, Phys. Rev. A **61**, 022504 (2000).
[7] W. A. van Wijngaarden, Can. J. Phys. **83**, 327 (2005).
[8] S. C. Pieper and R. B. Wiringa, Annu. Rev. Nucl. Part. Sci. **51**, 53 (2001).
[9] S. C. Pieper, V. R. Pandharipande, R. B. Wiringa, and J. Carlson, Phys. Rev. C **64**, 014001 (2001).
[10] G. Ewald, W. Nörtershäuser, A. Dax, S. Götte, R. Kirchner, H. J. Kluge, T. Kühl, R. Sanchez, A. Wojtaszek, B. A. Bushaw, G. W. F. Drake, Z. C. Yan, and C. Zimmermann, Phys. Rev. Lett. **93**, 113002 (2004); **94**, 039901 (2005).
[11] T. Udem, J. Reichert, R. Holzwarth, and T. W. Hänsch, Opt. Lett. **24**, 881 (1999).

[12] W. Scherf, O. Khait, H. Jager, and L. Windholz, Z. Phys. D: At., Mol. Clusters **36**, 31 (1996).
[13] J. Clarke and W. A. van Wijngaarden, Recent Res. Dev. Phys. **3**, 347 (2002).
[14] W. A. van Wijngaarden, Adv. At., Mol., Opt. Phys. **36**, 141 (1996).
[15] J. Walls, R. Ashby, J. J. Clarke, B. Lu, and W. A. van Wijngaarden, Eur. Phys. J. D **22**, 159 (2003).
[16] A. Beckmann, K. D. Bokle, and D. Elke, Z. Phys. **270**, 173 (1974).
[17] E. Arimondo, M. Inguscio, and P. Violino, Rev. Mod. Phys. **49**, 31 (1977).
[18] K. C. Brog, T. G. Eck, and H. Wieder, Phys. Rev. **153**, 91 (1967).
[19] L. Windholz, H. Jager, M. Musso, and G. Zerza, Z. Phys. D: At., Mol. Clusters **16**, 41 (1990).
[20] Z. C. Yan and G. W. F. Drake, Phys. Rev. Lett. **79**, 1646 (1997).
[21] H. Orth, H. Ackermann, and E. W. Otten, Z. Phys. A **273**, 221 (1975).
[22] C. Umfer, L. Windholz, and M. Musso, Z. Phys. D: At., Mol. Clusters **25**, 23 (1992).
[23] G. W. F. Drake, I. B. Khriplovich, A. I. Milstein, and A. S. Yelkhovsky, Phys. Rev. A **48**, R15 (1993).
[24] R. Mariella, Appl. Phys. Lett. **35**, 580 (1979).
[25] C. J. Sansonetti, B. Richou, J. R. Engleman, and L. J. Radziemski, Phys. Rev. A **52**, 2682 (1995).
[26] L. J. Radziemski, R. Engleman, and J. W. Brault, Phys. Rev. A **52**, 4462 (1995).
[27] B. A. Bushaw, W. Nörtershäuser, G. Ewald, A. Dax, and G. W. F. Drake, Phys. Rev. Lett. **91**, 043004 (2003).
[28] M. Goedfroid, C. F. Fischer, and P. Jonsson, J. Phys. B **34**, 1079 (2001).
[29] Z. C. Yan and G. W. F. Drake, Phys. Rev. A **66**, 042504 (2002).
[30] E. Riis, H. G. Berry, O. Poulsen, S. A. Lee, and S. Y. Tang, Phys. Rev. A **49**, 207 (1994).